Acta Cryst. (1976). A32, 799

Refinement of the Defect Structure of '$GeNb_9O_{25}$' by High-Resolution Electron Microscopy

BY A. J. SKARNULIS

Department of Chemistry, Arizona State University, Tempe, Arizona, U.S.A.

AND SUMIO IIJIMA AND J. M. COWLEY

Department of Physics, Arizona State University, Tempe, Arizona, U.S.A.

(*Received* 23 *January* 1976; *accepted* 18 *March* 1976)

It has been previously established that calculations of intensity distributions in high-resolution electron-microscope images of crystal structures can reproduce the experimental observations. The use of comparisons of observed and computed images for structure analysis has been extended for the first time to the refinement of a defect structure in the case of crystals of nominal composition '$GeNb_9O_{25}$'. The results show that previously proposed models for the disordered atom configurations around 'tetrahedral' sites are not completely correct. A new model is proposed which shows good agreement between computed and observed images. This model suggests an interpretation for observations on other related structures in terms of a new type of defect.

Introduction

In the past few years, the use of high-resolution microscopy to form two-dimensional images of crystal structures has become an increasingly powerful method for investigating crystal defects. A number of studies of linear and two-dimensional defects have been made and have been used in the investigation of the non-stoichiometry of transition metal oxide crystals and various minerals (Iijima, 1975). This development has been paralleled by theoretical calculations of image intensities (Fejes, 1973; Skarnulis, 1976; O'Keefe, 1973).

The usual basis for interpretation of the crystal structure images is the Cowley–Moodie formulation of the dynamical theory of electron diffraction. The effects of various electron optical parameters on the image contrast for well-ordered thin crystals have been investigated. For crystal thicknesses less than 100Å good agreement can be obtained between experimental and calculated images. Under optimum imaging conditions an intuitive interpretation of images is possible to some extent since the minima of intensity correspond to the positions of the heavier atoms in the projections of the crystal structure in the beam direction. However the information regarding crystal atom positions in crystal defects is not often obtained in such a direct, intuitive manner and for this purpose it is essential to make adequate calculations of intensities taking dynamical scattering effects fully into account.

In the course of studies of nonstoichiometric niobium oxide crystals, Iijima proposed that local dark contrast could be obtained from disorder in a column of atoms, parallel to the beam and only a few ångströms square, when the metal atoms are displaced in directions perpendicular to the beam (see Figs. 11, 12 and 13 of Iijima, 1973). In this way the spots observed in images of slightly oxidized $Nb_{12}O_{29}$ crystals were explained as being due to linear point-defect complexes which do not greatly perturb the surrounding host structure (Iijima, 1975). However, justification of this interpretation must be based entirely on theoretical calculations because the information in the images concerning such defects, which are extended in the beam direction, must be confined to variations of image contrast.

One of the main interests for the study of niobium oxides and related oxide systems is to determine the structural basis for their known nonstoichiometry. Allpress & Roth (1971) reported that intimate intergrowths of structure slightly different from that of the host crystal (Wadsley defects) may play an important role. Later one of the present authors (Iijima, Kimura & Goto, 1974) demonstrated experimentally that Wadsley defects may not be adequate to account for the nonstoichiometry in some cases but point defects may also exist. In particular, considerable fluctuations of contrast were observed at points corresponding to the presumed sites of tetrahedrally coordinated metal atoms in $Nb_{22+x}O_{54}$ crystals and it was concluded that these could indicate the presence of point defects in the related columns of atoms. Anderson, Bevan, Cheetham, Von Dreele, Hutchison & Strahle (1975) investigated '$GeNb_9O_{25}$' which has a structure related to that of $Nb_{22}O_{54}$ and concluded that the nonstoichiometry was associated with the presence of interstitial metal atoms around the tetrahedral sites. However the defect structure around these tetrahedral positions has not yet been convincingly explained.

The purpose of the present paper is to elucidate these defect structures by comparing calculated high-resolution electron-microscope image intensities with experimental observations. Various models for the atom configurations in the tetrahedral columns in the

crystals of '$GeNb_9O_{25}$' have been examined and the model giving best agreement with experiment has been determined.

Structure of '$GeNb_9O_{25}$'

The 'block structures' of such compounds as $Ti_2Nb_{10}O_{29}$, $Nb_{22}O_{54}$, $Nb_{12}O_{29}$, H–Nb_2O_5, *etc.* have been well established by X-ray diffraction (Wadsley & Andersson, 1970) and '$GeNb_9O_{25}$' belongs to this family. These structures are based on the ReO_3-type structure and have slabs of octahedra arranged in $n \times m$ blocks stacked infinitely in the third dimension (b axis is 3·8 Å). The characteristic crystal structure images of the block structure show dark contrast at the positions of metal concentration (*i.e.* shear planes) and white spots where there are empty columns or tunnels in the structures.

The structure of '$GeNb_9O_{25}$' as originally determined by X-ray diffraction, was assumed to be isostructural with PNb_9O_{25} (Roth, Wadsley & Andersson, 1965). This structure was found to be tetragonal with possible space groups of $I4$ or $I4/m$, which gave final R values of 9·2 and 9·3% respectively. Then Roth *et al.* chose $I4$ as the most likely space group because of the better temperature factors and their standard deviations. The parameters and positions used to calculate an image of the Roth *et al.* structure are shown in Table 1.

Table 1. *Crystallographic data for* '$GeNb_9O_{25}$' *(isostructural with* PNb_9O_{25}*) from Roth, Wadsley & Andersson* (1964)

System: tetragonal
Unit cell dimensions $a = 15{\cdot}60$ $c = 3{\cdot}838$ Å
Space group $I4$

	x	y	z	B
Ge	0	0·5	0·25	2·6 (1·1)
Nb(1)	0	0	0	1·3 (0·2)
Nb(2)	0·2188 (5)	0·1094 (5)	0	1·0 (0·1)
Nb(3)	0·1142 (5)	0·3310 (5)	0	0·9 (0·1)
O(1)	0	0	0·5	0·9 (1·7)
O(2)	0·2488 (32)	0·3917 (32)	0	0* (0·8)
O(3)	0·1121 (39)	0·0521 (37)	0	0* (0·7)
O(4)	0·1755 (41)	0·2212 (40)	0	1·4 (1·4)
O(5)	0·0175 (50)	0·2729 (50)	0	2·3 (1·5)
O(6)	0·0722 (50)	0·4531 (50)	0	2·3 (1·6)
O(7)	−0·1461 (34)	0·3536 (34)	0	0 (1·0)

* The least-squares refinement gave small negative values of B for these positions.

The structure of '$GeNb_9O_{25}$' itself was determined by Anderson *et al.* (1975) using both X-ray and neutron powder diffraction. The structure again had two possible space groups $I4$ or $I4/m$. Anderson's refinement gave better R values for $I4/m$ so that this space group was used. The final X-ray R value was 3·4% and the final neutron R value was 9·6%. Since the R value for the X-ray determination was better, their X-ray positions and occupancies were used to calculate an image on Anderson's model. The parameter and positions are presented in Table 2.

The '$GeNb_9O_{25}$' structure consists of 3×3 blocks of octahedra with tetrahedral positions near to each corner of each block (the hatched region of Fig. 1). Metal atoms in tetrahedral coordination lie at $y = \frac{1}{4}$ and $\frac{3}{4}$ along the short b axis (3·8 Å). At the corresponding points in the images there are usually heavy black spots (Fig. 6) but sometimes the contrast shows large variations.

Sample preparation

High-purity samples of GeO_2 and Nb_2O_5 (electronic and optical grade, 99·9+ purity) were mixed in the ratio 1:9 and sealed in a platinum tube which was heated to 1100°C for 24 h and then to 1325°C for 24 h. The furnace was allowed to cool to approximately 830°C and the sample was then removed and cooled to room temperature. The preparation appeared to be a single phase. Examination in the microsope confirmed the '$GeNb_9O_{25}$' structure. Wadsley defects consisting of insertions of $Nb_{22}O_{54}$-type structure were observed but formed an insignificant portion of the specimen.

Experimental procedure

The crystals were ground in an agate mortar and collected on a perforated carbon grid. The crystals were examined in the JEOL-100B electron microscope at 100 kV according to the procedure described elsewhere (Iijima, 1973). Thin crystal regions were sought and aligned with a goniometer stage so as to give a ($h0l$) reciprocal lattice section. All images were recorded by using an objective aperture with a radius of 0·392 $Å^{-1}$ in reciprocal space (position of the aperture is indicated by a circle in the electron diffraction pattern of Fig. 2). The divergence of the illumination

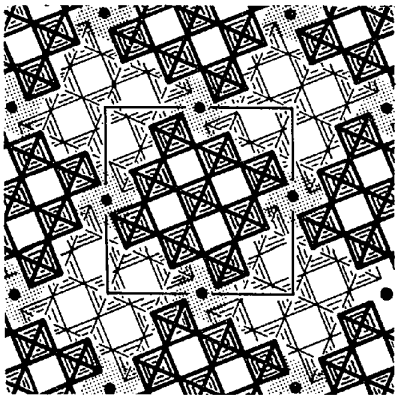

Fig. 1. Idealized model representing the structure of '$GeNb_9O_{25}$'. The darker and lighter squares which form 3×3 blocks of ReO_3-type structure by their corner sharing are centered about the two levels perpendicular to the b axis. The solid circles represent the tetrahedrally coordinated Nb or Ge atoms. Shaded areas are called 'tetrahedral column positions' in the text.

angle was $1{\cdot}2\times10^{-3}$ rad. The defocus values in the experimental images were estimated by assuming that the image taken under the condition where the amorphous carbon deposited at the edge of the crystal gave a minimum contrast corresponds to a defocus of about -250 Å.*

Calculations of image intensities were made by use of the slice method (Goodman & Moodie, 1974) based on the *n*-beam dynamical theory of Cowley & Moodie (1957). By use of an option of the program *DEFECT* (Skarnulis, Summerville & Eyring, 1976) it is possible to calculate an image for an imperfect crystal containing variations of structure in the beam direction. By this means calculations could be made for various models for the tetrahedral positions so that the composition of these regions, and so of the whole crystal, could be determined.

Description of the program

A complete discussion of program *DEFECT* is given by Skarnulis, Summerville & Eyring (1976). Corrections are included for spherical aberration, chromatic aberration, defocus and objective aperture sizes. The calculated images for the modified structures proposed in this paper were done using the 'interstitial or vacancy' option of the program, which allows one to calculate the projected potential of two different slice structures. One, the host structure, is the predominating structure for the crystal while the other, the defect structure, is intermingled with the host structure to generate the desired mixed crystal. In our case the host structure represents the '$GeNb_9O_{25}$' structure with only tetrahedral and no octahedral positions occupied within the columns containing the tetrahedral positions. The defect structure is the '$GeNb_9O_{25}$' structure (Anderson *et al.*, 1975) with no tetrahedral positions, but only the four octahedral positions occupied with one metal atom in each position. The program is completely flexible in allowing any sort of stacking sequence so it is possible to create a crystal of any composition and investigate the effect on the image by varying the projected potential in the third dimension. While the structures of the two types of slice are themselves unrealistic, superposition of a mixture of the two types of slice will give the same effect, in projection, as any desired occupancy of tetrahedral and octahedral sites.

Occupancy refinement

Using the option of program *DEFECT* (interstitial) described previously, a crystal was modeled by changing the stacking sequence in the third dimension to vary the projected potential. The slice thickness for the calculation was taken to be equal to the short *b* axis (3·8 Å). The experimental parameters used for the calculation were a spherical aberration constant $C_s=1{\cdot}8$ mm and an objective aperture radius of 0·210 $Å^{-1}$. According to O'Keefe & Sanders (1975), the divergence of the electron beam has the effect of reducing the aperture size in the back focal plane and so limiting the resolution. The objective aperture size first used was 0·263 $Å^{-1}$ which proved to be satisfactory for a thin crystal (5 slices = 19 Å) but very poor for thicker crystals (15 slices = 57 Å). To be consistent throughout the calculations, a value of 0·210 $Å^{-1}$ was used for the three crystal thicknesses.

Fig. 3 shows the calculated through-focus images for a crystal having a thickness of five slices. The first series of images is for the model described as isostructural with PNb_9O_{25} (Roth *et al.*, 1965), that is, the host structure for the series of calculations. The model contains only tetrahedrally coordinated germanium atoms. For this model the tetrahedral positions in the

* Defocus values were determined by observing an amorphous carbon film which is tilted at 45° to the direction of the incident beam. Firstly an image that has minimum contrast was found and then focus was changed by a known number of steps in objective current control knobs of the microscope. This makes the position of the band in which the minimum contrast has been observed shift by a certain distance perpendicular to the band. This distance divided by the number of the steps gives an amount of defocus corresponding to one step of the focusing control knobs.

Table 2. *Crystallographic data for* '$GeNb_9O_{25}$' *from Anderson, Bevan, Cheetham, Von Dreele, Hutchison & Strahle* (1975)

System: tetragonal
Unit cell dimensions $a=15{\cdot}736$ (3) $c=3{\cdot}827$ (1) Å
Space group $I4/m$

	x	*y*	*z*	*B*	$B_{11}(\times10^5)$	$B_{22}(\times10^5)$	$B_{33}(\times10^5)$	$B_{12}(\times10^5)$
Ge	0	0·5	0·25	0·42 (3)	31 (3)	31 (3)	2610 (100)	0·0
Nb(1)	0	0	0	0·42 (3)	62 (1)	62 (1)	6212 (81)	0·0
Nb(2)	0·21828 (2)	0·10546 (2)	0·0	0·42 (3)	39 (1)	83 (1)	438 (28)	−10 (1)
Nb(3)	0·11748 (2)	0·32574 (2)	0·0	0·42 (3)	66 (1)	104 (1)	717 (30)	−35 (1)
Nb(4)	−0·03003 (20)	0·44367 (22)	0·0	0·42 (3)	16 (10)	38 (10)	3936 (377)	−15 (6)
O(1)	0	0	0·5	1·68 (9)				
O(2)	0·2493 (1)	0·3883 (1)	0	0·62 (3)				
O(3)	0·1172 (2)	0·0495 (2)	0·0	0·87 (3)				
O(4)	0·1758 (2)	0·2156 (2)	0·0	0·96 (3)				
O(5)	0·0135 (2)	0·2814 (2)	0·0	0·98 (3)				
O(6)	0·0780 (2)	0·4454 (2)	0·0	0·90 (3)				
O(7)	−0·1595 (2)	0·3513 (2)	0·0	0·76 (3)				

optimum focus images (−600, −900 Å) show white spots. Similar results have been obtained by O'Keefe (1973). A calculation made with niobium occupying the tetrahedral positions showed the same results. The second series (Anderson *et al.* 1975) is for the X-ray single-crystal structural model of '$GeNb_9O_{25}$' with the parameters given in Table 2. This model contains not only tetrahedrally coordinated germanium and niobium atoms, which are supposed to be randomly distributed, but also niobium atoms in partially occupied octahedral sites. In this case the tetrahedral positions also show white spots. A calculation was made with the niobium atom completely occupying the tetrahedral positions with similar results. These results indicate that the images are insensitive to occupancy of the tetrahedral positions. It should be noted that these models fail to show the black spots at tetrahedral positions appearing in the experimental images for optimum defocus [Fig. 6(*e*), left] and therefore must be rejected.

Further calculations were made for models based on the Anderson *et al.* (1975) structure (hereafter referred to as JSA) (JSA0 to JSA3) by use of the 'interstitial' option of program *DEFECT*. The numbers 0 to 3 refer to the number of 'defect' slices having fully occupied octahedral positions which are intermingled with the host structure to give a total of five layers. With two such defect slices (JSA2; eight octahedrally coordinated metal atoms and three tetrahedrally coordinated metal atoms) the white spots in the images at the tetrahedral positions disappear. With the addition of a third such slice (JSA3), these positions become darker than the bands along the shear planes, as observed experimentally.

The quite rapid change of the spots at the tetrahedral positions from white to black allows the number of these slices containing octahedral positions, which is required to obtain agreement with experimental observations, to be estimated with an accuracy of approximately ±0·5. This in turn allows the minimum concentration of metal atoms in octahedral coordination to be estimated.

Similar sets of calculations to show the change of intensity at tetrahedral sites were made for thicknesses of 10 slices (38 Å) and 15 slices (60 Å) (Fig. 4) with much the same results. To obtain the best value for the metal atom concentrations, the number of defect slices required to give adequate contrast at the tetrahedral positions was plotted against crystal thickness. The plotted points fell closely on a straight line through the origin. The slope indicated an average occupancy for the octahedral sites of approximately 0·5 metal atoms per unit cell, independent of crystal thickness.

For the calculations of Fig. 3 (JSA2) it was assumed that within the tetrahedral column there are eight occupied octahedral metal sites and three atoms in tetrahedral sites. This number of metal atoms cannot be fitted reasonably into the available sites, but since the intensity at the tetrahedral column positions is known to be almost independent of the number of tetrahedral sites occupied we can consider fewer tetrahedral sites to be occupied without changing the results.

Models of the defect structures

In describing the defect structures around the tetrahedral sites indicated by hatched areas in Fig. 1 we use the simplified representations indicated in Fig. 5(*a*). In this diagram of the tetrahedral column for '$GeNb_9O_{25}$' the tetrahedrally coordinated metal atom sites are indicated by triangles and the octahedral sites are indicated by diamonds. There are two groups of octahedral sites, one at $z=0$ (labelled O) and one at $z=\frac{1}{2}$ (labelled O'). Occupied sites are indicated by solid triangles or diamonds. For the original structure of Roth, Wadsley & Andersson (1965) for PNb_9O_{25}, the tetrahedral sites are all occupied, on average, by half an atom and all octahedral sites are empty.

Fig. 5(*b*) shows a model for the column occupancy proposed by Anderson *et al.* (1975). Table 3 shows the corresponding metal to metal distances in the column. The most important feature of this model is that it does not contain any close pairs of occupied octahedral positions. This seems chemically reasonable but, as we have seen, it cannot account for the observed black spots in the image.

As we mentioned earlier, the lattice image calculations give an estimate of the number of metal atoms located in the octahedral sites within the tetrahedral column necessary to produce a black contrast that

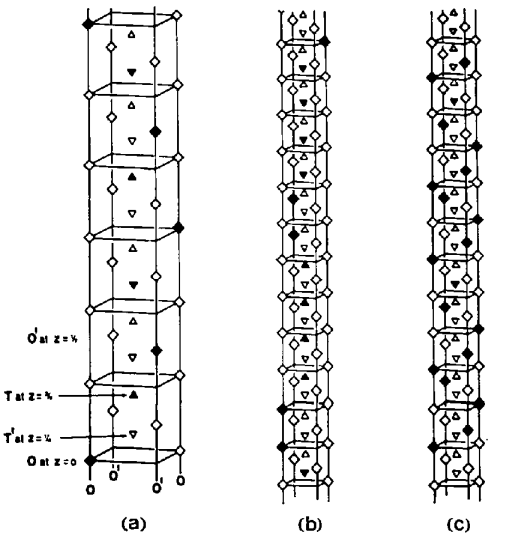

Fig. 5. (*a*) Schematic drawings representing the atomic arrangements within a tetrahedral column corresponding to the shaded areas in Fig. 1. Triangles and diamonds represent tetrahedral sites (T, T') and octahedral sites (O, O') respectively and filled symbols indicate occupancy. (*b*) A model for the ordered occupation sequence in the tetrahedra column proposed by Anderson *et al.* (1975). (*c*) A modified model proposed in the present study.

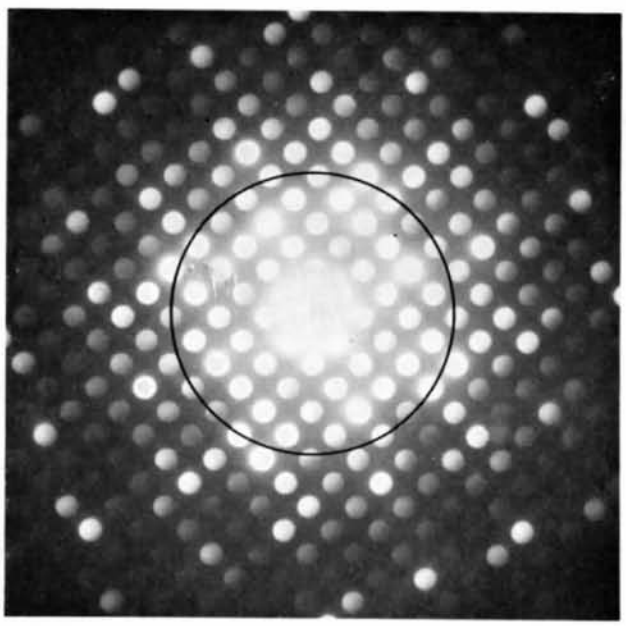

Fig. 2. An electron diffraction pattern from a crystal of '$GeNb_9O_{25}$'. From the spread of the spots an actual illumination angle on the specimen has been measured ($1{\cdot}2 \times 10^{-3}$ rad). A circle indicates the position of the objective aperture and reflections inside the circle contribute to the image.

[*To face p.* 802

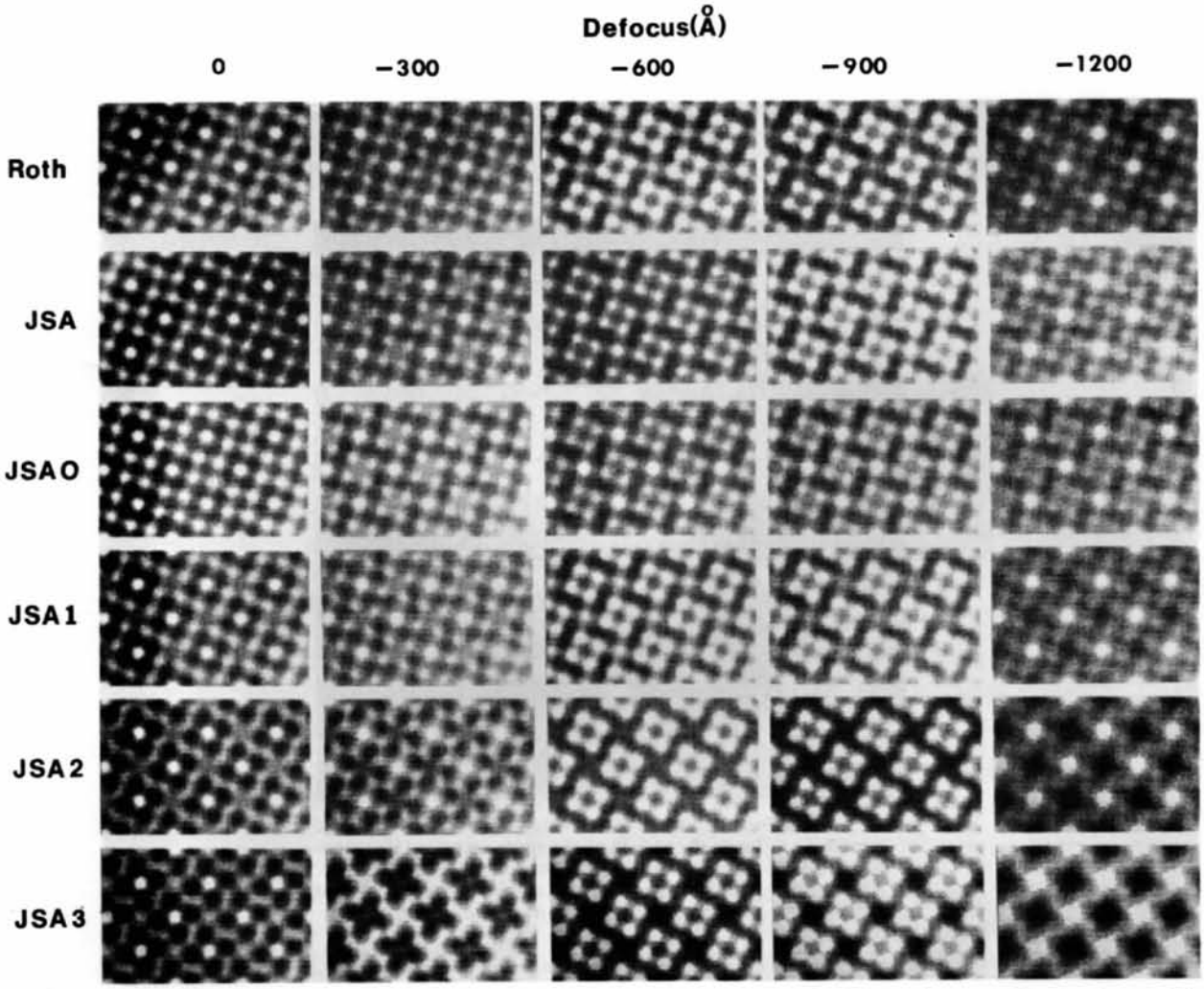

Fig. 3. Calculated through-focus lattice images of the crystal of '$GeNb_9O_{25}$'. Crystal thickness is assumed to be about 19 Å (5 slices). Roth refers to images obtained by using structure data given by Roth, Wadsley & Andersson (1965) for PNb_9O_{25}. JSA refers to images obtained by using structure data given by Anderson *et al.* (1975). JSAO–JSA3 are images obtained by using modified structures of JSA. 0–3 indicate the number of the defect layers (see text.) From variations in the contrast of the calculated images at the tetrahedral column positions (see Fig. 1) at −600 Å defocus, a best-fit model was determined by comparison of the experimental images from various models.

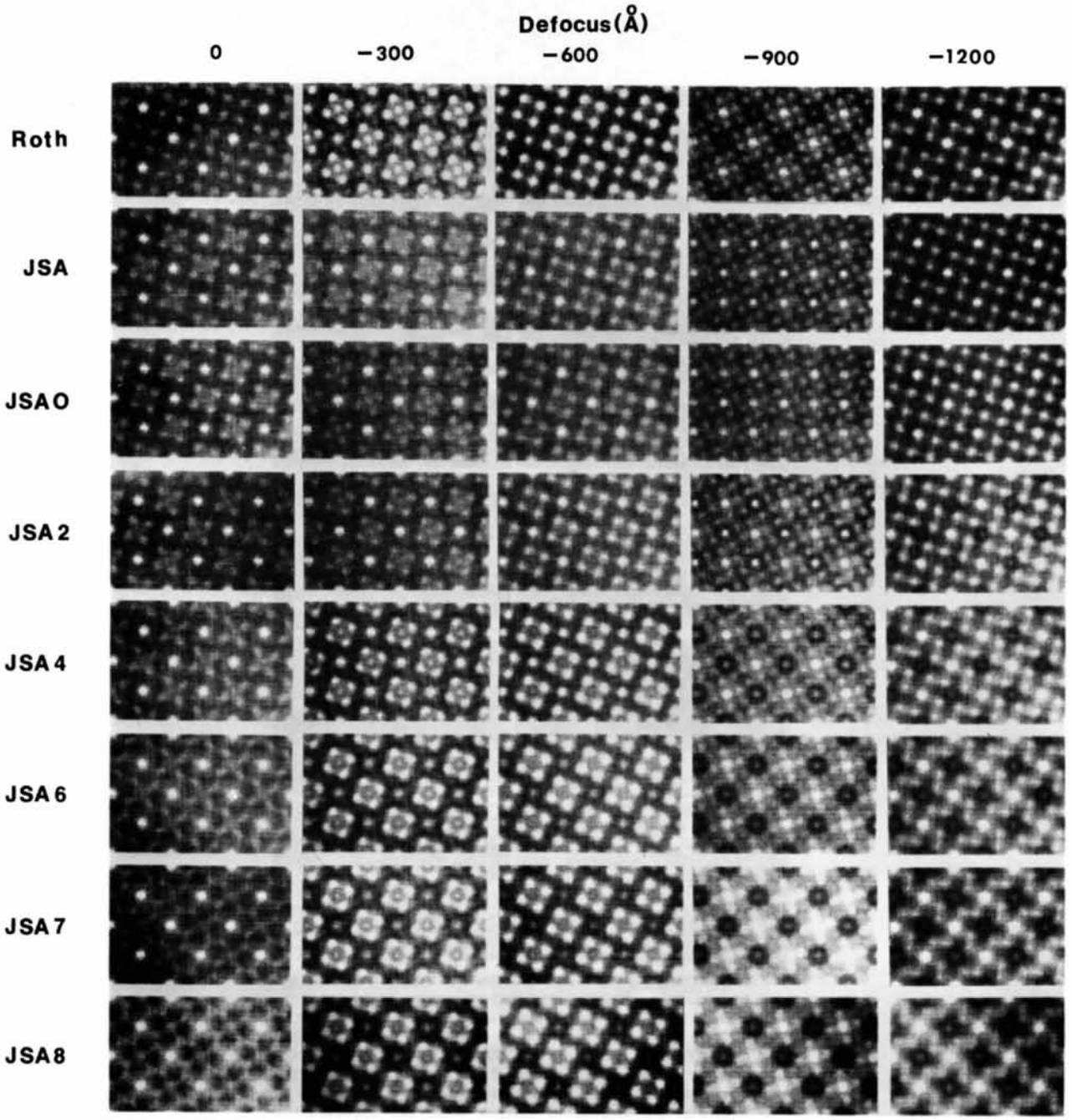

Fig. 4. Calculated through-focus lattice images similar to those in Fig. 3 but crystal thickness is assumed to be 57 Å (15 slices).

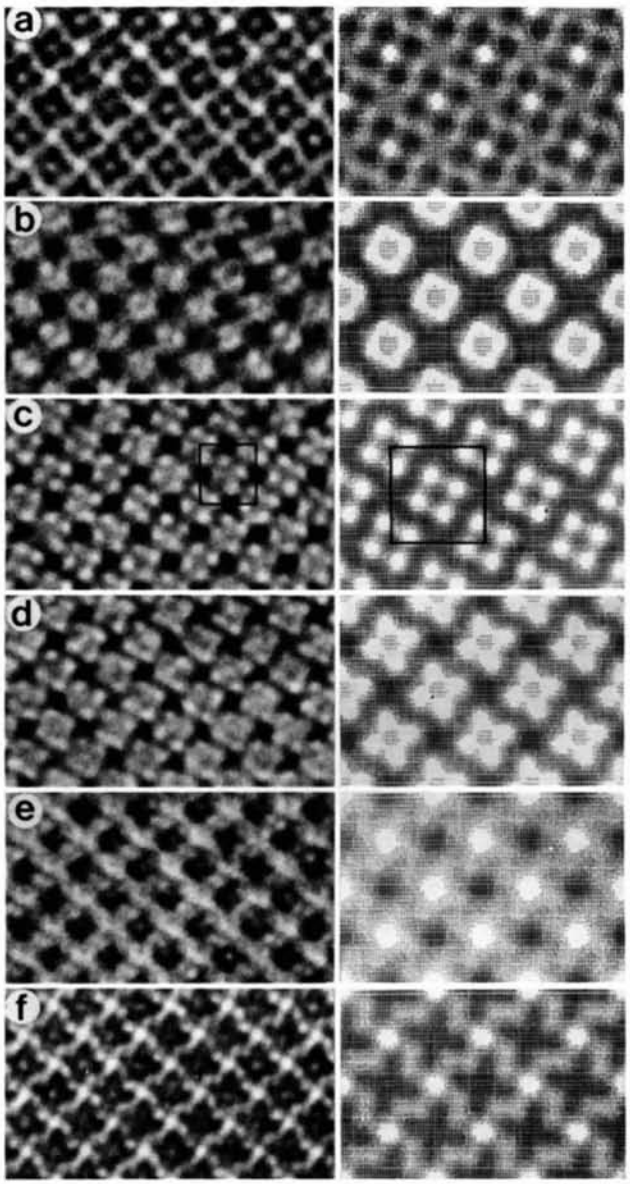

Fig. 6. Comparison of experimental through-focus images (left column) with calculated best-fit images (right column). Defocus values for experimental and theoretical images are: (*a*) −100, −100 Å (*b*) −450, −425 Å (*c*) −700, −700 Å (*d*) −950, −975 Å (*e*) −1200, −1175 Å (*f*) −1500, −1500 Å, respectively. Structural data used for the calculation are those from the refined structure (JSA2) obtained by comparing the calculated images with the experimental images. The image in (*c*) is the 'optimum defocus' image, which is directly compared with the structure (Fig. 1).

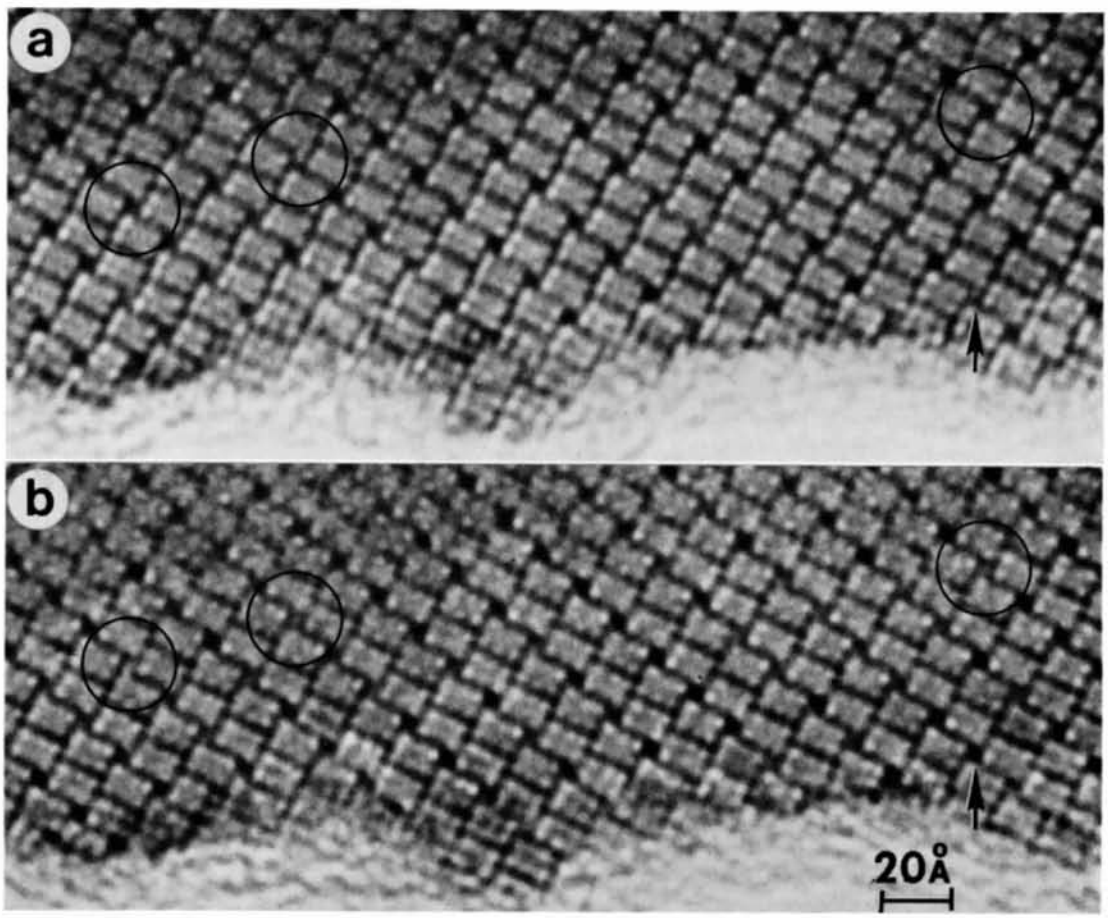

Fig. 7. Effect of the electron beam irradiation on the contrast at the tetrahedral column positions. (*a*) At an initial stage and (*b*) after 5 min. The successive images were taken from the crystal of $Nb_{25}O_{62}$ with a slight excess of metal. Note that the dark contrasts [circles in (*a*)] become lighter in (*b*) or *vice versa* (arrowed).

was observed in the experimental images but the calculations do not tell the exact locations of the metal atoms in the octahedral sites.

It is also obtained that the occupancy of the tetrahedral positions by either Nb or Ge makes almost no contribution to the image contrast of the tetrahedral column positions. Therefore an actual model for the defect structure to fulfill the conditions mentioned above cannot be uniquely determined. One of many possible models for the JSA2 which could be made by varying the stacking sequence of the pairs of filled octahedral sites and the tetrahedral sites is shown in Fig. 5(*c*), which is based on the JSA model. In order to accommodate more metal atoms into the octahedral sites than those in the JSA model we ignore the restrictions of the JSA and place metal atoms in pairs of neighboring octahedral sites. The separation of the pairs of occupied octahedral sites (2·38 Å) is then less than for other pairs in the structure but is not unreasonable.

The composition of the model of JSA2 can be estimated on the basis of the comparison of calculated and observed intensities.

The positions of the metal atoms along the tetrahedral columns cannot be determined because the image corresponds to a projection of the structure. Hence we can assume the metal atoms to be distributed among two different types of slices, each one unit cell thick. One type of slice contains only one tetrahedral atom, assumed to be Ge with the rest of the structure intact and no octahedral sites in the tetrahedral column occupied. This slice has the composition $[Ge]Nb_9O_{25}$ where the brackets include the metal atom content of the column. The other type of slice has two of the octahedral sites within the column occupied by metal atoms, assumed to be Nb. One of these metal atoms replaces the atom in the tetrahedral site of the Roth model. The other is assumed to come from outside the column, leaving a vacancy in the remainder of the slice, so that the composition of the slice is $[Nb_2]Nb_8O_{25}$.

Here it is assumed that a total of four octahedrally coordinated metal atoms come from outside the column because the amount of excess metal atoms would seem extremely large and that for electrical neutrality it would require even a larger excess of oxygen. The model has an average composition of $Ge_{0\cdot2}Nb_{9\cdot8}O_{25-\alpha}$ which contains 98 mol% of Nb_2O_5. α represents the number of oxygen vacancies necessary for charge balance. In this case there is one vacancy per five slices of crystal or one vacancy per tetrahedrally coordinated Ge. The range of composition of our model would be from six to eight metal atoms occupying the octahedral positions giving an average composition of $Ge_{0\cdot4}Nb_{9\cdot6}O_{25-\alpha}$ to $Ge_{0\cdot2}Nb_{9\cdot8}O_{25-\alpha}$ with $\alpha=2$ vacancies per Ge(T) position at the low end to one vacancy per Ge(T) at the high end.

Considering the fact that Anderson *et al.* (1975) used excess GeO_2 (7·2:1 of Nb_2O_5 to GeO_2) and got only 7·6 mol% of GeO_2 in the crystal the small uptake of Ge does not seem very surprising. Also the model of octahedrally occupied metals with oxygen vacancies agrees quite well with the density measurements made by Kimura (1975) on the other types of models proposed for the defects in this type of system.

Through-focus image series

Examination of the full set of images in a through-focus series allows a more complete test of the structural model we have derived. Although the images obtained away from the optimum defocus cannot be directly interpreted in terms of atom configurations, they provide additional comparisons of observed and calculated intensities and are, if anything, more sensitive to small discrepancies in the assumed models. This has been demonstrated in the comparisons of experimental and calculated images for crystals of $4Nb_2O_5.9WO_3$ (Skarnulis & Iijima, 1975).

A further reason for using the through-focus series is that for the purposes of the refinement of structures by use of high-resolution images, which we have attempted here for the first time, it is necessary to be as accurate as possible in the determination of the experimental parameters. It is well known that the image contrast varies critically with such experimental parameters as the crystal orientation and thickness, and the defocus, astigmatism and mechanical stability of the microscope. A through-focus series obtained under carefully controlled conditions can help to avoid ambiguities in the assignment of defocus values and provide a wealth of experimental data.

One criterion for the reliability of images is that the image symmetry should not change with crystal thickness. This is particularly useful for the detection of small deviations from an exact zone-axis orientation. The effects of small deviations of the crystal orientation can be strongly enhanced by dynamical effects to give pronounced perturbations of the contrast in

Table 3. *Metal–metal distances*

These are quoted from Anderson *et al.* (1975). Atom numbers refer to positions listed in Table 2.

Nb(1)–Nb(2)	3·8147 (4) Å	Nb(4)–Ge (at $z=1\cdot25$)	4·890 (4) Å
Nb(2)–Nb(3)	3·8120 (4)	Nb(4)–Nb(3)	2·973 (6)
Nb(2)–Nb(3′)	3·3903 (4)	Nb(4)–Nb(4′)	2·003 (9)
Nb(4)–Ge (at $z=0\cdot25$)	1·385 (5)	Nb(4)–Nb(4″)	2·381 (5)
Nb(4)–Ge (at $z=0\cdot75$)	3·040 (5)	Nb(4)–Nb(4) (at $z=1\cdot0$)	3·830 (1)

(′) refers to a position on the same layer.
(″) refers to octahedral positions in the tetrahedral column.

thick-crystal regions. The observation of symmetry in the electron diffraction pattern intensities, which is normally used for determining the orientation of the crystal, may be a less sensitive indication of alignment because the pattern usually comes from a relatively large area and may be affected by bending or other distortion of the crystal.

For many of the oxide structures, it is known that relatively thick regions of the crystal may show a repetition of the good thin-crystal images (Fejes, Iijima & Cowley, 1973). The possibility of observing these thick-crystal images depends critically on the crystal orientation. In the present case, the alignment of the beam with the [010] zone axis must be very precise.

Fig. 6 shows an experimental through-focus series of images for '$GeNb_9O_{25}$', obtained under nearly perfect imaging conditions (left-hand column), compared with the theoretically calculated series (right-hand column). The estimated crystal thickness is about 30 Å. The structure used for the calculation was that derived above, having two defect slices in the thickness of five slices (19 Å). The values for the defocus of the experimental images were obtained from a calibration of the microscope but are subject to some degree of uncertainty. Therefore images were calculated for small steps of defocus to determine the best fit between calculated and observed intensities.

As noted before, the image calculated for optimum defocus shows a direct representation of the projection of the structure in the incident beam direction, in agreement with experiment. Over the whole through-focus series, the agreement is satisfactory. This provides further confirmation of our proposed model for the defect structure around the tetrahedral positions and supports the conclusion that previously proposed models are unacceptable.

One further observation may be made regarding the through-focus series. The experimental images (*a*) and (*f*) appear to be reversals of the optimum defocus image (*c*). This may be associated with a reversal of the contrast (a phase change of π) for the stronger reflections, as in the Fourier images for simple structures (Cowley & Moodie, 1957). However the details of the images, especially for the calculated ones, show that this reversal relationship is only approximate, as might be anticipated.

Discussion

The results of the analysis of the atom configurations in '$GeNb_9O_{25}$' have significance for the understanding of other structures. The images of crystals of $Nb_{22}O_{54}$ which have a slight excess of metal atoms show considerable fluctuations in the contrast at the tetrahedral positions (Iijima, Kimura & Goto, 1974). Similar results have been observed in images of crystals of $Nb_{25}O_{62}$ which also have a slight excess of metal (Fig. 7). The images (Fig. 7*a*,*b*) were taken of the same part of a crystal but the image in Fig. 7(*b*) was recorded after several minutes of electron beam irradiation. It is interesting to note that in such a series of pictures the dark contrast at the tetrahedral column positions may change during the electron beam irradiation. At the points indicated by circles the dark contrast decreases and almost disappears. At points such as that indicated by an arrow, the process is reversed.

Anderson *et al.* (1975) reported electron microscope images '$GeNb_9O_{25}$' crystals in which the tetrahedral column positions at very thin regions of the crystal were imaged as white spots. Similar images were also observed in our specimen. Such white spots may arise because, for an extremely thin crystal the maximum number of the octahedrally coordinated atoms in the tetrahedral columns may be not enough to generate black contrast at the tetrahedral column positions. The relative fluctuation in the number of the metal atoms in the octahedral sites becomes greater, and this can give variable or asymmetrical contrast distributions in the tetrahedral column positions. For a relatively thicker crystal, as shown in Fig. 6 (about 30 Å), the distribution of the metal atoms becomes more uniform in the tetrahedral columns, giving less fluctuation in the contrast at these positions.

In conjuction with these considerations we may also note the related case of the defect structure observed in crystals of $Nb_{12}O_{29}$ having a slight excess of oxygen (Iijima, Kimura & Goto, 1973). The dark spots appearing within the block structures in this case were attributed to linear chains of point defect clusters and a structural relationship with the defects around tetrahedral sites in other structures seems probable.

The explanation given, without theoretical justification, (Iijima, 1975) was in terms of the displacement of metal atoms from normal octahedral sites to either interstitial octahedral sites [as indicated by O or O′ in Fig. 5(*a*)] or to tetrahedral sites [indicated by *T* in Fig. 5(*b*)]. A configuration resembling that of the tetrahedral columns in other structures could then be generated and would produce the dark spots in the image.

The theoretical calculations of images described in this paper have given support to our previously hypothetical model for the defects occurring in the tetrahedral columns and furthermore they have allowed us to discuss the defect structures in a more quantitative manner. A conclusion of importance for the discussion of the previously observed defects is that the occurrence of dark spots at the tetrahedral positions does not necessarily imply an excess of metal atoms there. This was already indicated by the observation that the dark spots may become lighter and this change is reversible (Fig. 7). It is not reasonable to explain this observation in terms of the migration of metal atoms over long distances because the diffusion rate for metal atoms in the block structures is very low. However it should be relatively easy for metal atoms to move between the tetrahedral sites (*T*) and the octahedral sites (*O*)

within the tetrahedral columns. The refinement we have made of the defect structure has clearly shown that such small movements can generate the dark contrast at the tetrahedral column positions.

In relation to this conclusion, it may be noted that in most structure images obtained before from the various types of block structures, the tetrahedral column positions usually showed black spots. This suggests that much the same type of disorder as that proposed here for the metal atoms within the tetrahedral columns may occur in many related crystals. Such disorder may account for the large R values which have commonly been obtained for the tetrahedral atoms in crystal structure analyses of block structures. We therefore suspect that this disorder in the tetrahedral columns may be associated with their nonstoichiometry. In fact the presence of such defects in addition to Wadsley defects has been indicated experimentally (Allpress & Roth, 1971; Iijima, Kimura & Goto, 1974).

For a complete discussion of the nonstoichiometry of the block structures we should also consider the oxygen lattice. One indication on this question is that the metal atom displacements giving the black spot contrasts in $Nb_{12-x}O_{29}$ appear to be associated with the presence of excess oxygen atoms (Iijima, Kimura & Goto, 1973). This suggests the possibility of some disorder in the oxygen atom positions around the tetrahedral columns in '$GeNb_9O_{25}$' which in our case seems to be oxygen vacancies, although Anderson *et al.* (1975) concluded that the oxygen lattice is perfect and the nonstoichiometry results only from the distribution of interstitial metal atoms. Unfortunately the contribution of the oxygen atoms to the image contrast is small, because of the relatively small scattering power of oxygen, and it is unlikely that disorder in the configuration of oxygen atoms in these materials will be detectable in the near future.

We thank Drs R. S. Roth, A. E. Cheetham and R. B. Von Dreele for stimulating discussions. This work was supported by NSF Grant GH36668 and GH37477.

References

ALLPRESS, J. G. & ROTH, R. S. (1971). *J. Solid State Chem.* **3**, 209–216.

ANDERSON, J. S., BEVAN, D. J. M., CHEETHAM, A. E., VON DREELE, R. B., HUTCHISON, J. L. & STRAHLE, J. (1975). *Proc. Roy. Soc.* A**346**, 139–156.

COWLEY, J. M. & MOODIE, A. F. (1957). *Proc. Phys. Soc.* B**70**, 497–504.

FEJES, P. L. (1973). Ph.D. Thesis, Arizona State Univ.

FEJES, P. L., IIJIMA, S. & COWLEY, J. M. (1973). *Acta Cryst.* A**29**, 710–714.

GOODMAN, P. & MOODIE, A. F. (1974). *Acta Cryst.* A**30**, 280–290.

IIJIMA, S. (1973). *Acta Cryst.* A**29**, 18–24.

IIJIMA, S. (1975). *Acta Cryst.* A**31**, 784–790.

IIJIMA, S., KIMURA, S. & GOTO, M. (1973). *Acta Cryst.* A**29**, 632–636.

IIJIMA, S., KIMURA, S. & GOTO, M. (1974). *Acta Cryst.* A**30**, 251–257.

KIMURA, S. (1975). Private communication.

O'KEEFE, M. A. (1973). *Acta Cryst.* A**29**, 389–401.

O'KEEFE, M. A. & SANDERS, J. V. (1975). *Acta Cryst.* A**31**, 307–310.

ROTH, R. S., WADSLEY, A. D. & ANDERSSON, S. (1965). *Acta Cryst.* **18**, 643–647.

SKARNULIS, J. (1976). Ph.D. Thesis, Arizona State Univ.

SKARNULIS, J. & IIJIMA, S. (1975). Unpublished.

SKARNULIS, J., SUMMERVILLE, E. & EYRING, L. (1976). *Acta Cryst.* To be published.

WADSLEY, A. D. & ANDERSSON, S. (1970). *Perspectives in Structural Chemistry*. Vol. III, pp. 1–58.